EUROPEAN ORGANIZATION FOR NUCLEAR RESEARCH (CERN)

CERN-PH-EP-2014-061
LHCb-PAPER-2014-014
April 10, 2014

Observation of the resonant character of the $Z(4430)^-$ state

The LHCb collaboration

SUPPLEMENTAL PLOTS APPROVED FOR PUBLIC PRESENTATIONS

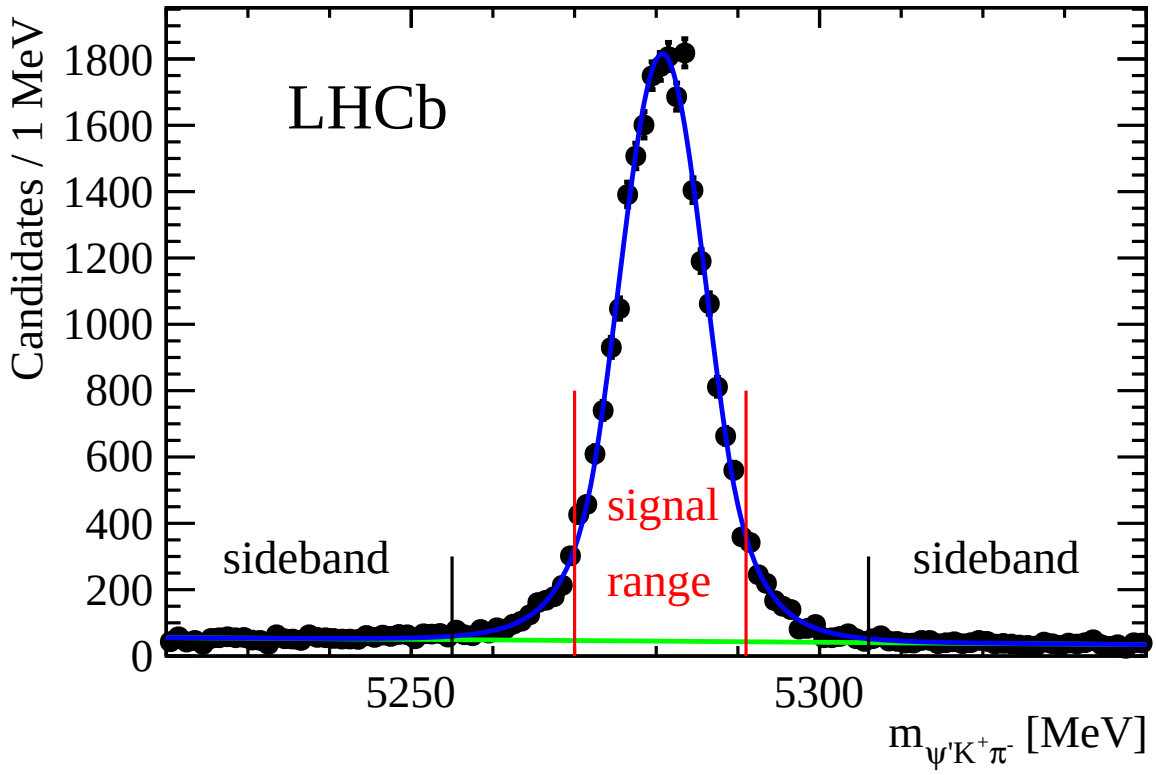

Figure 1: Invariant mass distribution of the $B^0 \to \psi' K^+\pi^-$ candidates. The fit (blue line) of a double-sided symmetric Crystal Ball signal shape and linear background (green line) are superimposed. The fit gives 25176 ± 174 signal and 5383 ± 102 background events in the fitted range. The fitted mass resolution is $\sigma = 5.35 \pm 0.05$ MeV. Vertical red lines show the signal region used in the amplitude fit, $5270 < m_{\psi' K^+\pi^-} < 5291$ MeV (about $\pm 2\sigma$ around the peak). Smaller vertical black lines indicate boundaries of the sidebands used for the background parameterization in the amplitude fit, $5220 - 5255$ MeV and $5306 - 5340$ MeV. The background fraction in the signal region is $(4.1 \pm 0.1)\%$.

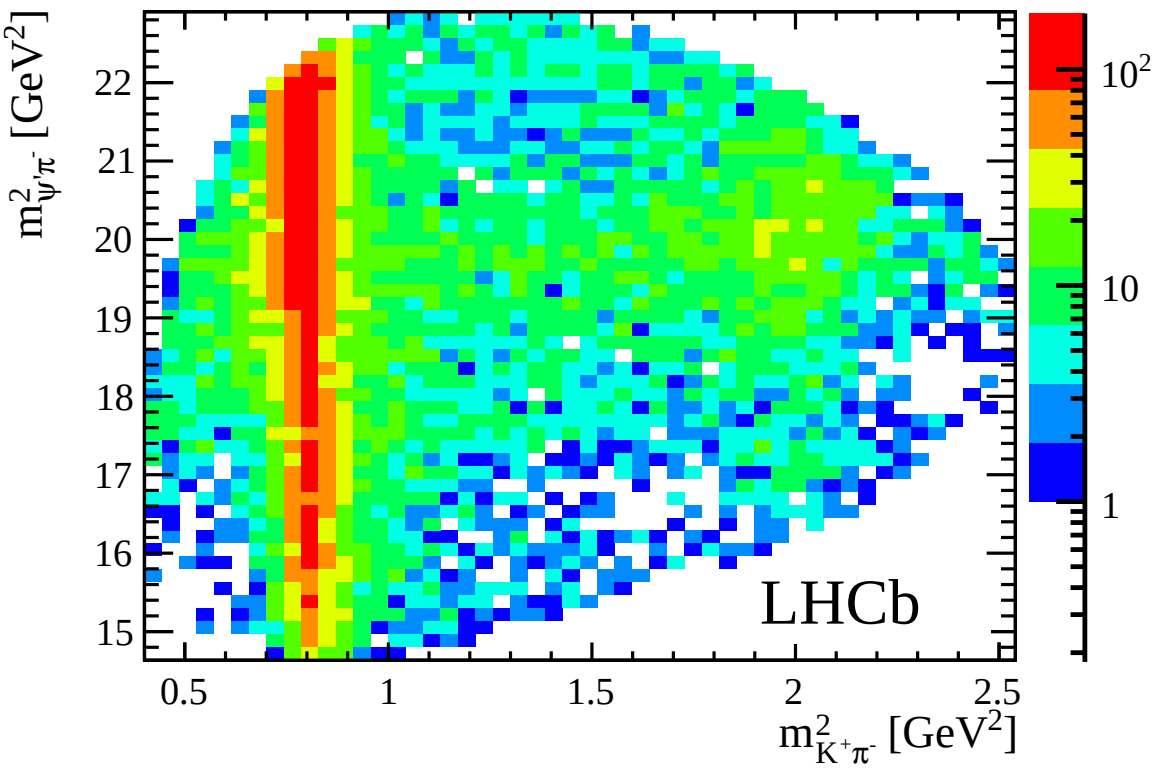

Figure 2: Dalitz plot for $B^0 \to \psi' K^+\pi^-$ candidates. The background has been subtracted using sWeights determined by the fit shown in Fig, 1. The colors indicate number of signal events per bin. The dominant vertical band is due to the $K^*(892)$ resonance. A faint vertical band at $m^2_{K^+\pi^-}$ around 2 GeV^2 is due to the $K^*_2(1430)$ peak. A horizontal $Z(4430)^-$ band is also visible ($m^2_{\psi'\pi^-}$ around 20 GeV^2).

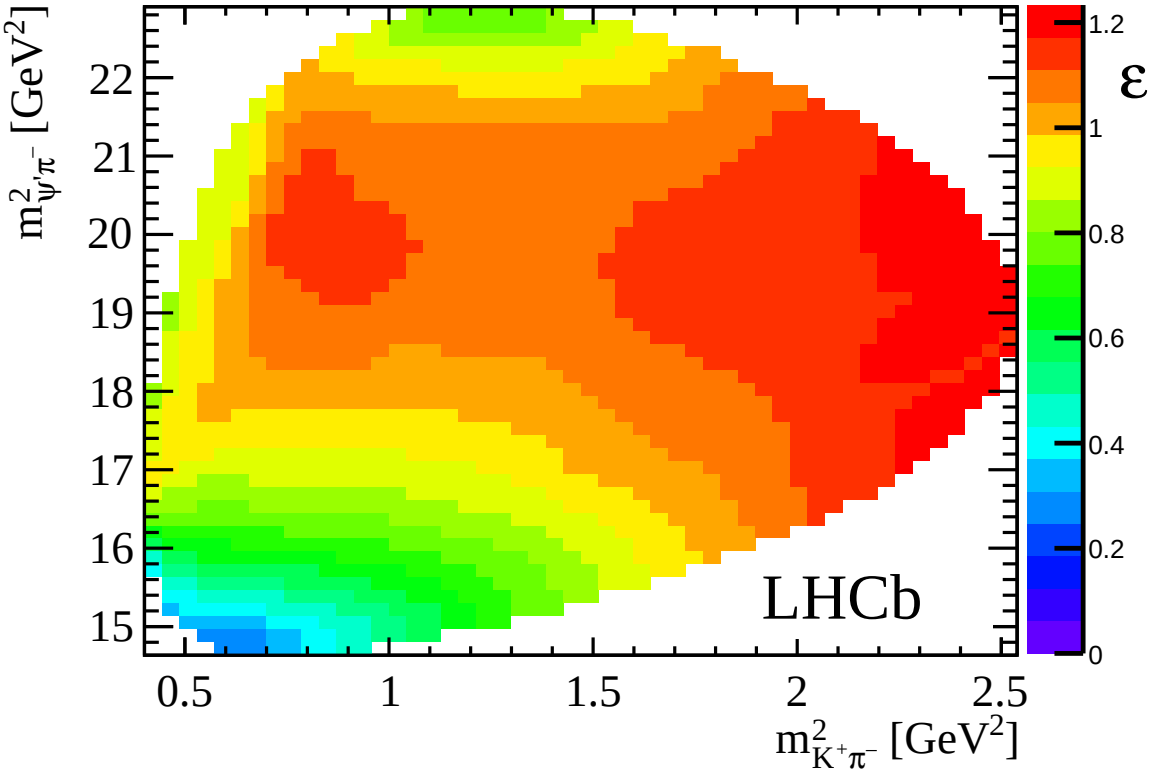

Figure 3: Relative variation of the selection efficiency for $B^0 \to \psi' K^+\pi^-$ candidates across the Dalitz plane. Average efficiency over the Dalitz plane is unity by the definition.

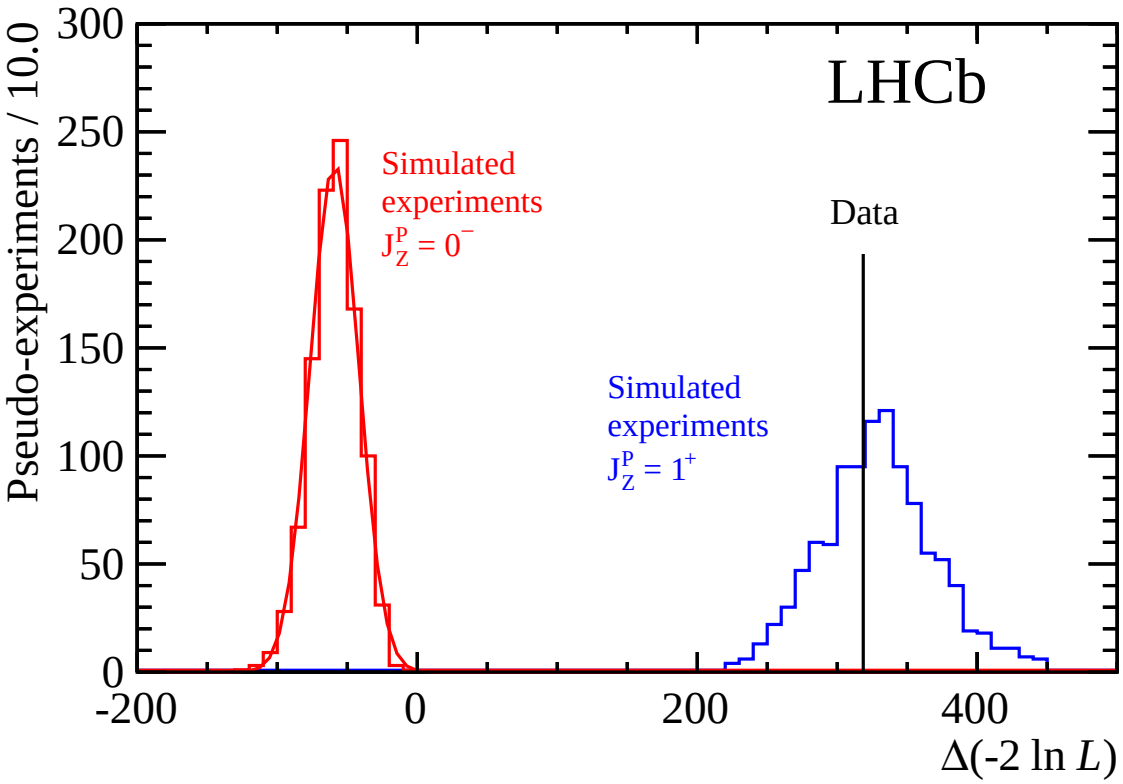

Figure 4: Distribution of $\Delta(-2\ln L) = [-2\ln L(0^-)] - [-2\ln L(1^+)]$ for pseudoexperiments generated according to the amplitude fit to the real data with $Z(4430)^-$ set to the $J^P = 0^-$ (red histogram) or $J^P = 1^+$ (blue histogram) hypothesis, each fit with the disfavored (0^-) and with the favored (1^+) spin hypothesis. Following the approach of the Belle collaboration [1] we fit an asymmetric Gaussian function to the simulated $J^P = 0^-$ distribution (superimposed) and integrate it above the value of $\Delta(-2\ln L)$ obtained with the real data sample (indicated with a vertical black line), which gives a p-value for the $J^P = 0^-$ hypothesis equivalent to 25.7σ. Such a large rejection level is expected according to the simulated $J^P = 1^+$ distribution; probability of obtaining this rejection level, or higher, is 61%.
Compare with Fig. 9 of Ref. [1].
Relying on the asymptotic (*i.e.* valid for large data sample) theorem for separate hypotheses, a lower limit on the rejection level for the $J^P = 0^-$ hypothesis is $> 17.8\sigma$, as obtained by integrating a $\chi^2(\text{ndf} = 1)$ distribution (not shown here) above the data value. The simulations shown here justify the use of this asymptotic theorem on our data sample. The final rejection levels in the spin analysis are obtained by looking for the lowest rejection calculated using the asymptotic bound method among the systematic variations of the fit model.

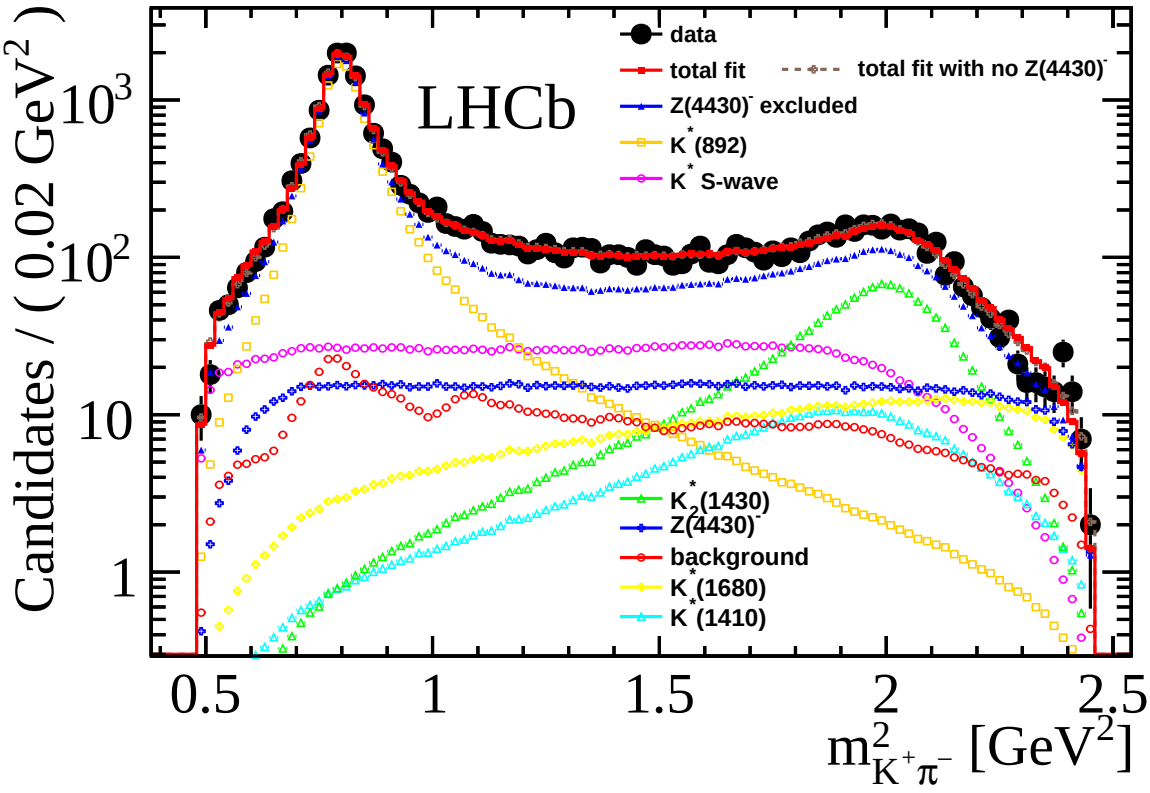

Figure 5: Distribution of $m^2_{K^+\pi^-}$ with the projections of the 4D amplitude fit superimposed. The vertical scale is logarithmic. The fit with no $Z(4430)^-$ (brown dashed histogram) essentially overlaps the fit with $Z(4430)^-$ (red solid histogram), therefore, it is hard to see. The same as top-right Fig.2 in the publication, except the legend has been added.

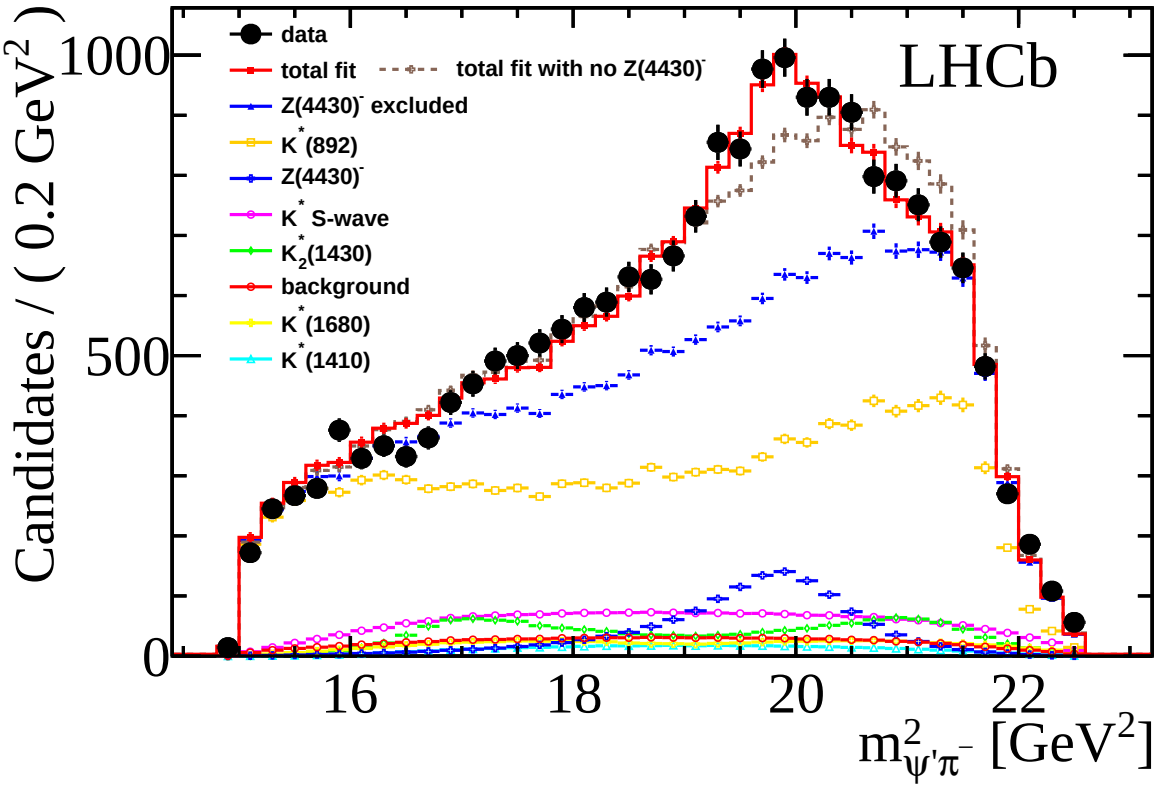

Figure 6: Distribution of $m^2_{\psi'\pi^-}$ with the projections of the 4D amplitude fit superimposed. The same as top-left Fig.2 in the publication, except the legend has been added. Four different $m_{K^+\pi^-}$ slices of the distribution shows here are shown in Fig. 7-11.

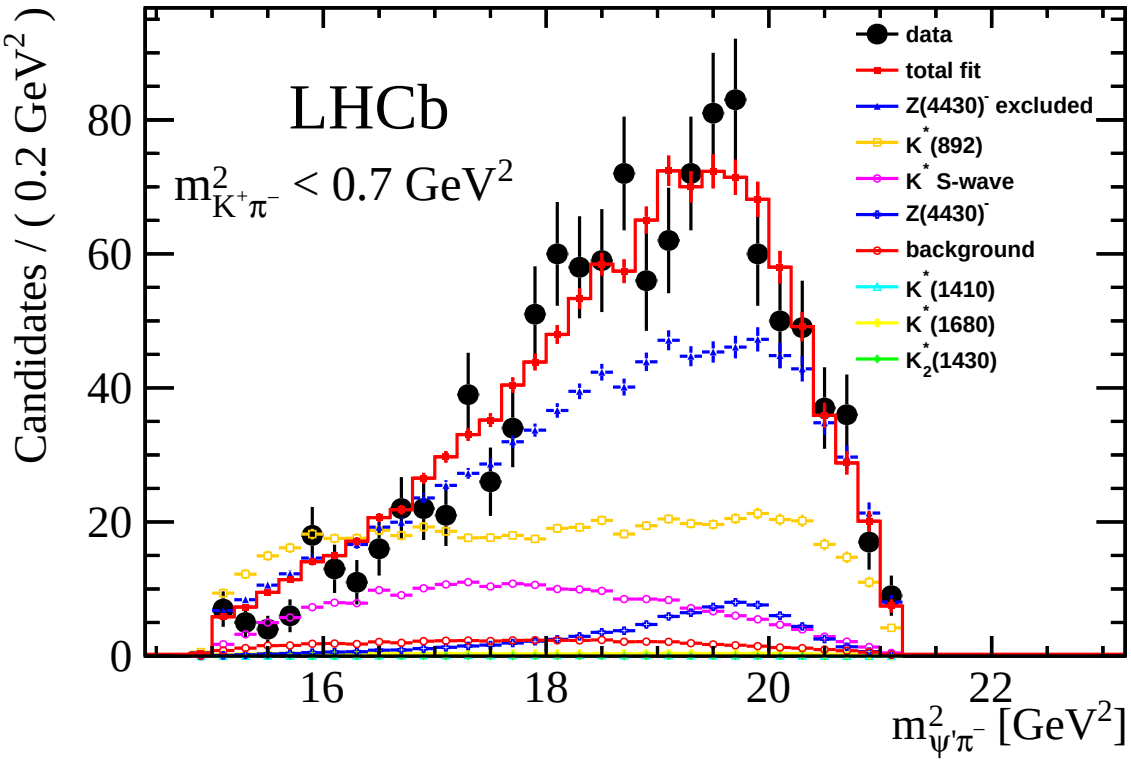

Figure 7: Distribution of $m^2_{\psi'\pi^-}$ for the $m_{K^+\pi^-}$ region below the $K^*(892)$ resonance with the projections of the 4D amplitude fit superimposed.

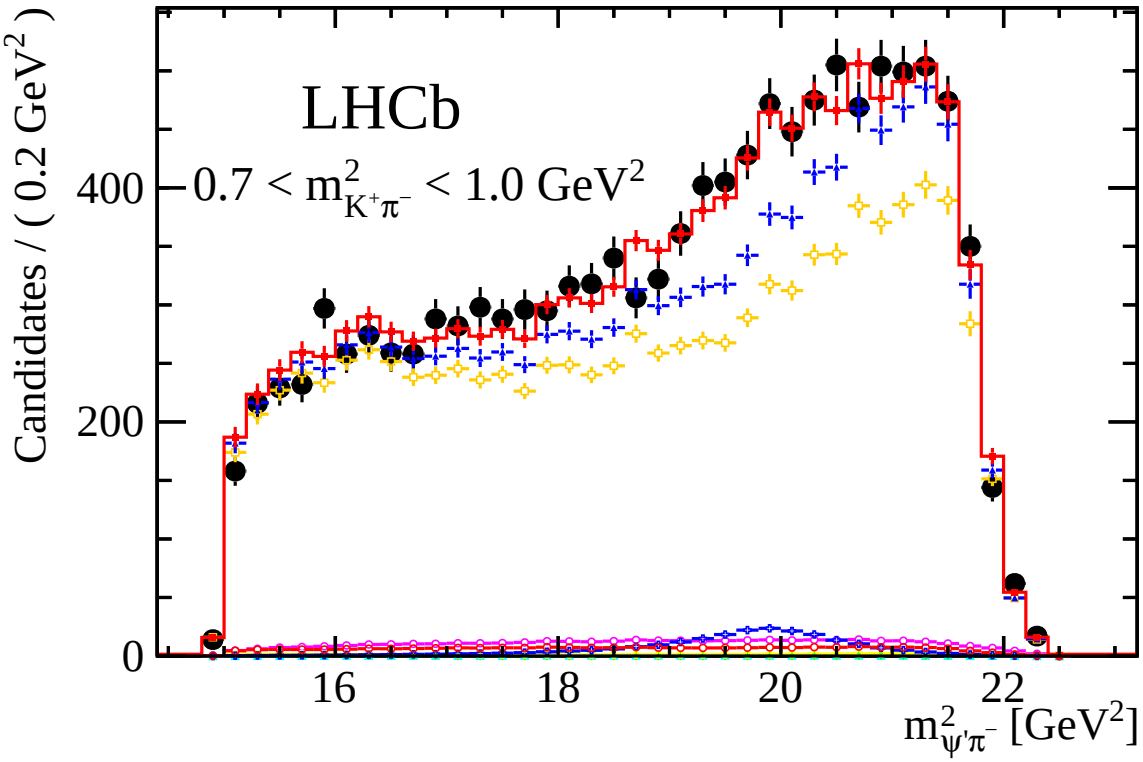

Figure 8: Distribution of $m^2_{\psi'\pi^-}$ for the $m_{K^+\pi^-}$ region at the $K^*(892)$ resonance peak with the projections of the 4D amplitude fit superimposed. See Fig. 7 for the legend.

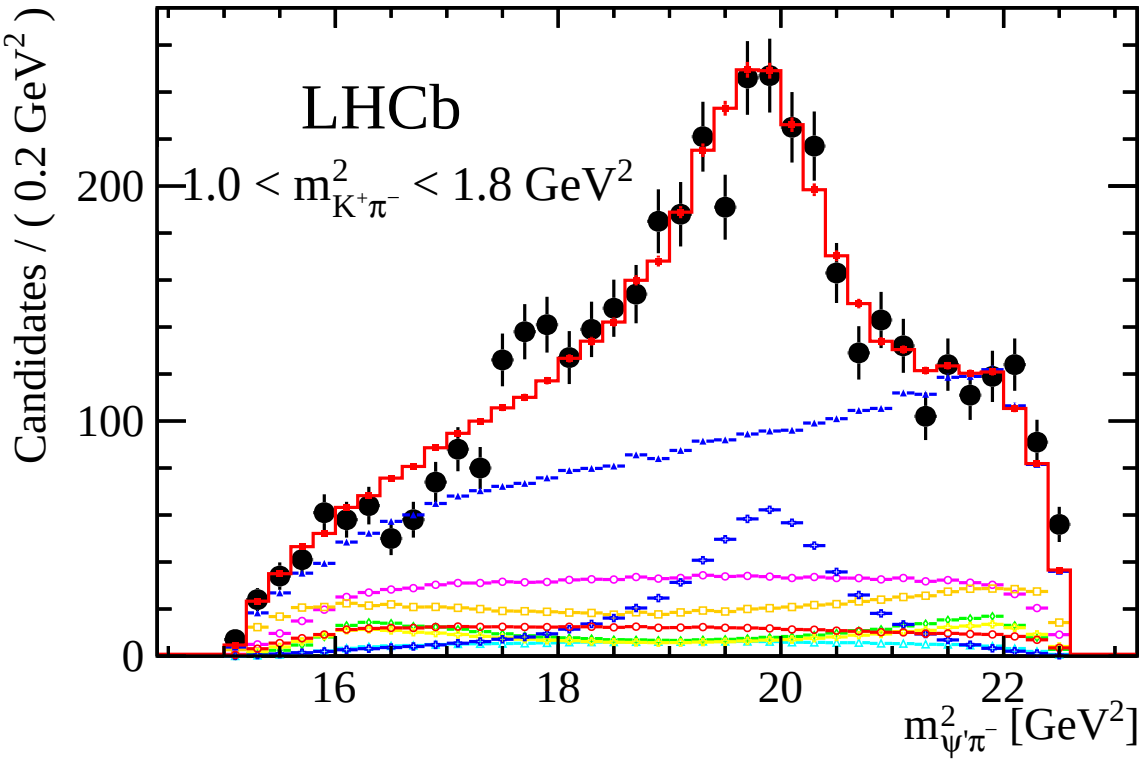

Figure 9: Distribution of $m^2_{\psi'\pi^-}$ for the $m_{K^+\pi^-}$ region in the central part of the Dalitz plot between the two dominant K^* resonances, $K^*(892)$ and $K^*_2(1430)$ (called "K^* veto region" in the Belle papers), with the projections of the 4D amplitude fit superimposed. See Fig. 7 for the legend. The same data are displayed in Fig. 4 of the publication, where the default fit with $Z(4430)^-$ displayed here is compared to the fit with the $Z(4430)^-$ and an additional 0^- Z^- state at a lower mass. Compare to Fig. 13 for the fit with no Z^- at all.

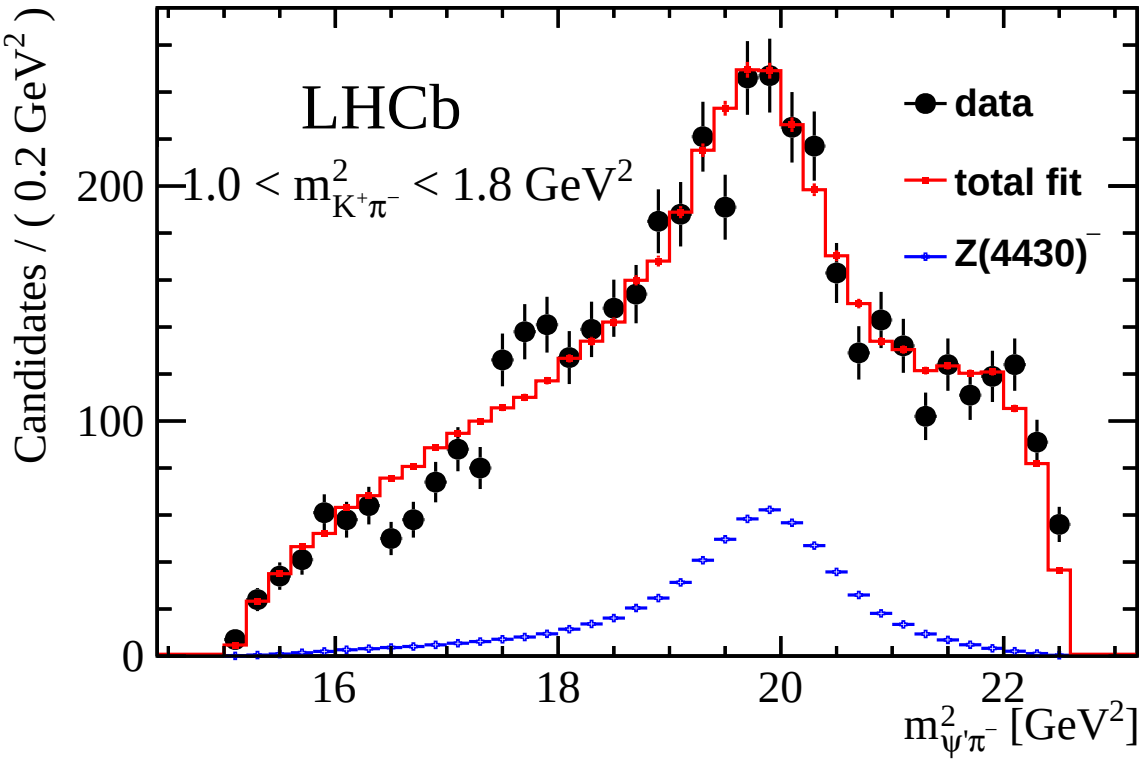

Figure 10: Same as Fig. 9 but individual K^* components in the fit are not shown.

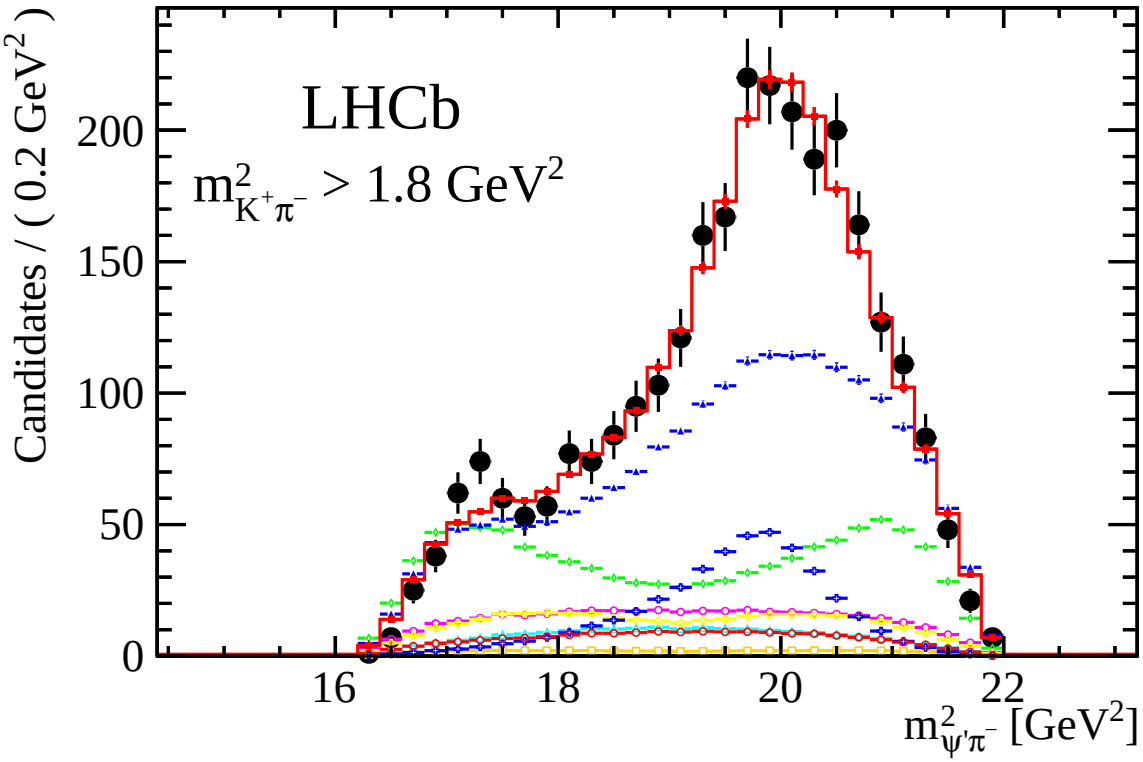

Figure 11: Distribution of $m^2_{\psi'\pi^-}$ for the $m_{K^+\pi^-}$ at the $K^*_2(892)$ resonance peak region and above, with the projections of the 4D amplitude fit superimposed. The vertical scale is logarithmic. See Fig. 7 for the legend.

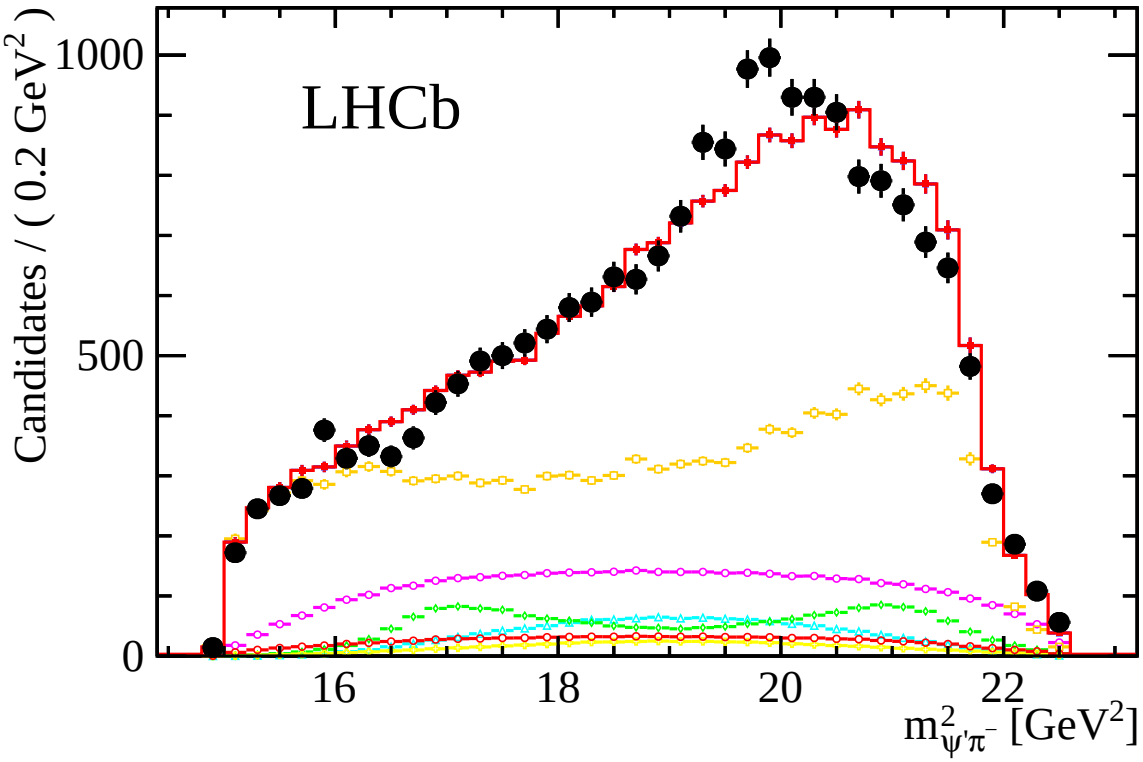

Figure 12: Distribution of $m^2_{\psi'\pi^-}$ with the projections of the 4D amplitude fit without $Z(4430)^-$ superimposed. A slice of the distribution shows here, for the $m_{K^+\pi^-}$ region suppressing the dominat K^* resonances is shown in Fig. 13.

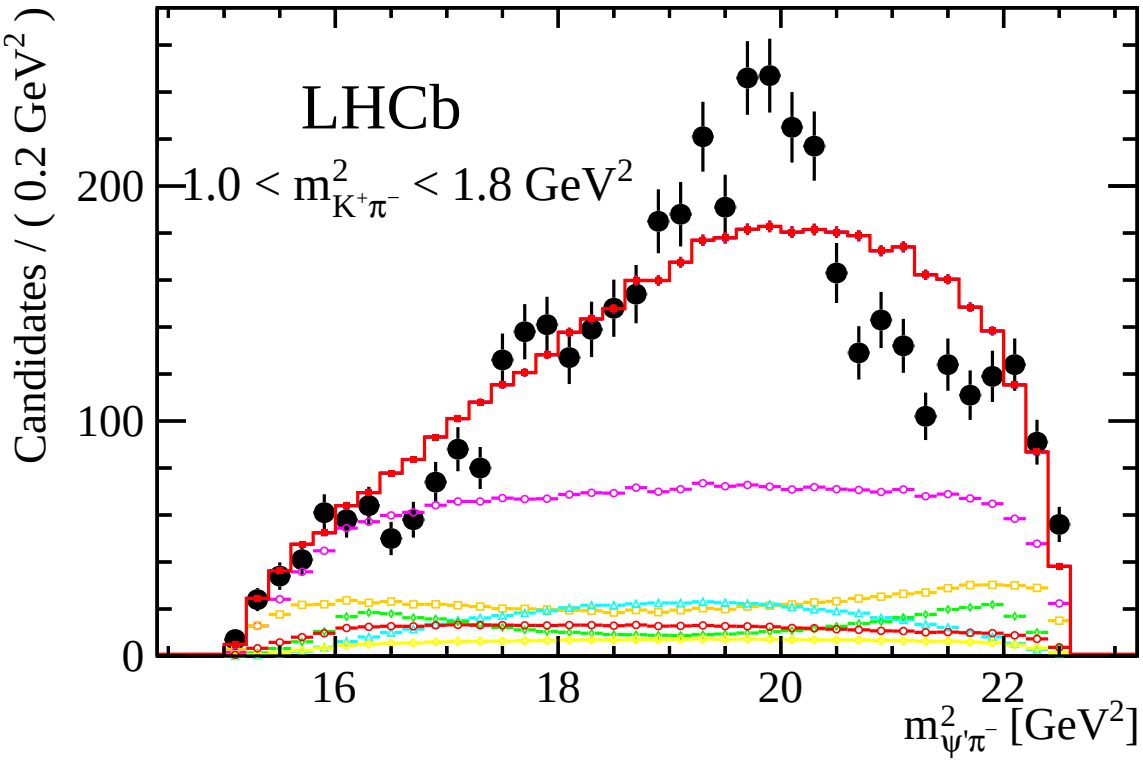

Figure 13: Distribution of $m^2_{\psi'\pi^-}$ for the $m_{K^+\pi^-}$ region in the central part of the Dalitz plot between the two dominant K^* resonances, $K^*(892)$ and $K^*_2(1430)$ (called "K^* veto region" in the Belle papers), with the projections of the 4D amplitude fit without $Z(4430)^-$ superimposed. See Fig. 7 for the legend. Compare to Fig. 9 for the fit with $Z(4430)^-$ or Fig. 4 in the publication for the fit with two Z^-s.

References

[1] Belle collaboration, K. Chilikin *et al.*, *Experimental constraints on the spin and parity of the* $Z(4430)^+$, Phys. Rev. **D88** (2013) 074026, arXiv:1306.4894.